Electronic structure of the naphthalene radical cation and some simple alkylated derivatives

Thomas Bally,*[a] Claudio Carra,[a] Markus P. Fülscher[b] and Zhendong Zhu†[a]

[a] *Institut de Chimie Physique de l'Université, Perolles, CH-1700 Fribourg, Switzerland*
[b] *Department of Theoretical Chemistry, Chemical Centre, POB 124, S-22100 Lund, Sweden*

The excited states of the radical cations of naphthalene (N), dihydroacenaphthylene (A) and pyracene (P) are probed experimentally by photoelectron (PE) and by electronic absorption (EA) spectroscopy. Their electronic structure is discussed in some detail on the basis of *ab initio* CASSCF/CASPT2 calculations which yield a description in good accord with experiment, both with regard to band positions and intensities. For example, they help to explain why a prominent band in the EA spectrum of $N^{\bullet+}$ is absent in the spectra of $A^{\bullet+}$ and $P^{\bullet+}$. This is not due to a spectral shift induced by the alkyl bridges, but rather to a cancellation of transition dipole moments that is only partial in $N^{\bullet+}$ but more complete in the two derivatives. It is found that—in spite of the relatively small relaxation energies of the vertically formed radical cations—the accompanying geometry changes on ionization may lead to quite substantial shifts in some of the excited state energies, notably that of the first (unobserved) one. Therefore, the common assumption that the good correlation between the PE spectra of polycyclic aromatic hydrocarbons and the EA spectra of their radical cations is due to the rigidity of these compounds is not well founded.

Introduction

Radical cations of polycyclic aromatic hydrocarbons have recently been the focus of much attention following their detection in outer space. They are thought to give rise to some of the enigmatic diffuse interstellar bands,[1] which has led to detailed spectroscopic investigations of those species in the laboratory, in particular by matrix isolation techniques. The radical cation of naphthalene ($N^{\bullet+}$), the simplest of these species, has been studied by gas phase UV–photoelectron (UP),[2] photodissociation (PD)[3,4] and zero-kinetic-energy (ZEKE) photoelectron spectroscopy,[5] as well as by electron paramagnetic resonance (EPR) spectroscopy in $CFCl_3$ and ZSM-5 Zeolite,[6] by electronic absorption (EA) spectroscopy in organic glasses,[7] in solution[8] and in noble gas matrices,[9–11] as well as by infrared (IR) spectroscopy,[11,12] also in noble gas matrices.

These experimental data have also been modelled by various quantum chemical procedures. The vibrational structure of ground-state $N^{\bullet+}$ appears now to be quite well understood,[4] but most calculations of excited state energies and transition moments have been restricted to various semi-empirical methods[13–15] whose results did not always agree.[15] To the authors' best knowledge, only two *ab initio* calculations on $N^{\bullet+}$ have been reported.[16,17] In this paper we present the first consistent picture of the electronic structure of $N^{\bullet+}$, both for the neutral and the cation geometries, based on *ab initio* CASPT2 calculations which have proven to give very reliable predictions of excited states of aromatic hydrocarbons,[18] and, more recently, also radical cations.[17,19,20] We also examined the effect of alkyl substitution by including in the study the two dimethylene-bridged derivatives, dihydroacenaphthylene ($A^{\bullet+}$) and pyracene ($P^{\bullet+}$).

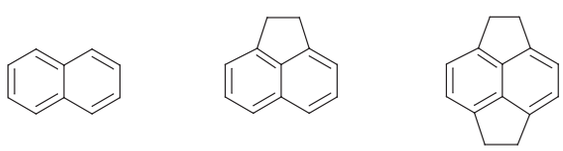

N A P

† *Present address:* Department of Chemistry, The Ohio State University, Columbus, OH 43210, USA.

Experimental and computational methods

Compounds

Naphthalene was purchased from Fluka and used without further purification. Samples of dihydroacenaphthylene and pyracene were kindly provided by Professor Jakob Wirz (University of Basel) and were used after sublimation.

Experimental

The radical cations of the three hydrocarbons were produced by X-irradiation of samples matrix-isolated at 12 K in argon containing an equimolar amount of CH_2Cl_2 as an electron scavenger, as described previously.[21] Whereas naphthalene could be statically pre-mixed with argon in the desired ratio, the reduced volatility of the alkyl derivatives required that they be placed in a U-tube and carried along by an argon stream flowing over them at reduced pressure. EA spectra were measured on a Perkin-Elmer Lambda 19 instrument. The PE spectra were recorded on a modified Perkin-Elmer PE 16 instrument operated in preretardation (and hence constant resolution) mode[22] under computer control. Calibration was effected with a Xe–Ar mixture and the spectral resolution was about 12 meV (digital resolution 2 meV).

Theoretical

The geometries of the three hydrocarbons were optimized within the D_{2h} (**N** and **P**) or C_{2v} point group (**A**) by the B3LYP/6-31G* hybrid density functional method[23] using the GAUSSIAN program.[24] Excitation energies and transition moments were computed by the CASSCF/CASPT2 method[25] as implemented in the MOLCAS program,[26] using atomic natural orbital (ANO) type basis sets[27] contracted to split-valence plus polarization (SVP) quality.‡ Because radical cations are

‡ Cartesian coordinates of B3LYP/6-31G* optimized geometries of **N**, **A** and **P**, as well as their radical cations, CASSCF and CASPT2 total energies for all excited states listed in Tables 1–3 are available as supplementary material (SUPPL. NO. 57398, 5 pp.). For details of the Supplementary Publications Scheme see 'Instructions for Authors', *J. Chem. Soc., Perkin Trans. 2*, available *via* the RSC Web page (http://www.rsc.org/authors). The supplementary data is also available on the RSC's web server (http://www.rsc.org/suppdata/perkin2/1998/1759/).

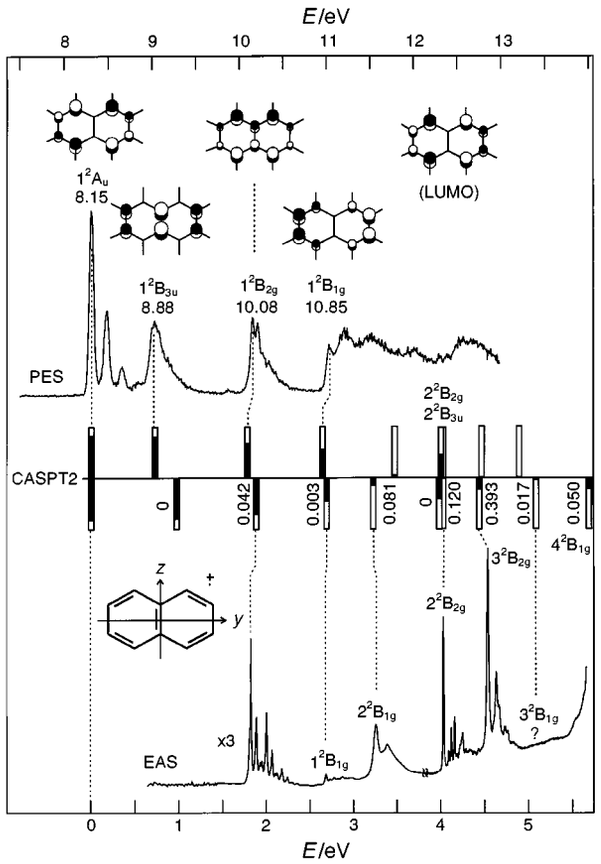

Fig. 1 Photoelectron spectrum (PES) of naphthalene and electronic absorption spectrum (EAS) of the corresponding radical cation, plotted on a common energy scale whose origin for the EAS coincides with $I_{v,i}$ in the PES. The bars in the center represent the results of the CASPT2 calculations listed in Table 1. The black shading is proportional to the Koopmans character of the different excited states (for discussion see text) and the numbers next to the bars pointing down denote oscillator strengths for electronic transitions.

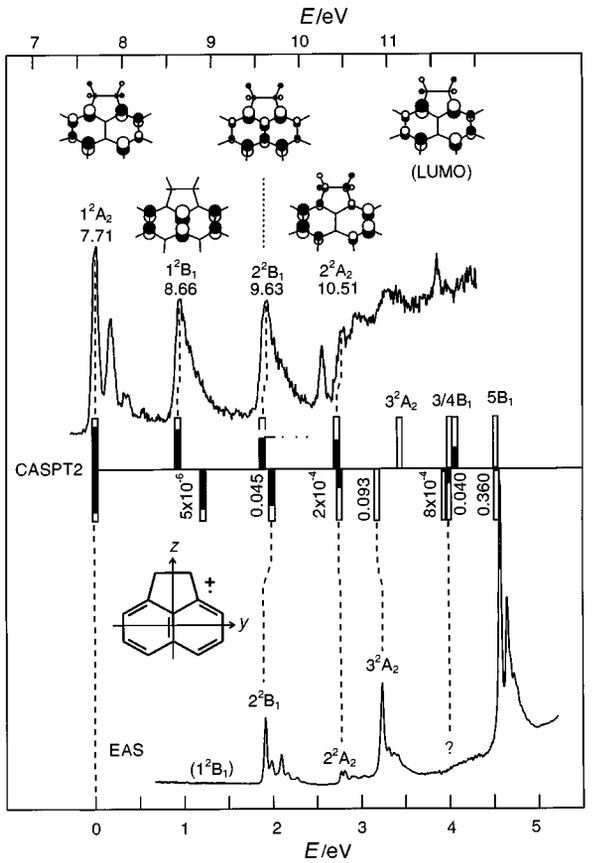

Fig. 2 Photoelectron spectrum (PES) of pyracene (**P**) and electronic absorption spectrum (EAS) of the corresponding radical cation, along with a representation of the CASPT2 results listed in Table 2. For explanations, see caption to Fig. 1.

electron deficient, the wave functions are sufficiently compact at low excitation energies that interactions with Rydberg states are negligible. Earlier calculations on polyene radical cations had shown that adding higher angular momentum functions to the basis set has no influence on the results.[19]

CASSCF wave functions were obtained using the state averaging technique (all states were equally weighted). Thus, all states of a given symmetry are described by a common set of molecular orbitals. The active space included the ten valence π-orbitals localized at the naphthalene group (five occupied and five virtual MOs) and nine electrons. Exploratory, large CASSCF calculations for $\mathbf{P}^{\bullet+}$ including thirteen electrons in fourteen orbitals showed that none of the alkyl bridge orbitals affected the excitation energies or the composition of the wave functions in any significant way.

To compute the dynamic correlation contribution to the state energies, the carbons' core orbitals were kept frozen. Initially, calculations on the high lying states of $\mathbf{A}^{\bullet+}$ and $\mathbf{P}^{\bullet+}$ were hampered by weakly interacting intruder states. The latter were removed by applying a level shift of 0.25 hartree (changing this value by ±0.05 hartree resulted in no significant change in the excitation energies and shows that no artefacts were introduced by this measure). The final CASPT2 wave functions were described to 68–71% ($\mathbf{N}^{\bullet+}$), 65–67% ($\mathbf{A}^{\bullet+}$) and 60–63% ($\mathbf{P}^{\bullet+}$) by the CASSCF reference function. Finally, oscillator strengths were computed by combining the transition dipole moments and excitation energies calculated on the basis of the CASSCF and CASPT2 wave functions, respectively.

Results and discussion

Figs. 1–3 show the PE spectra of the three compounds juxtaposed with the EA spectra of the corresponding radical cations on a common energy scale. For the EA spectra, the origin of this scale is coincident with $I_{v,i}$ in the PE spectra which can be readily discerned in the case of polycyclic aromatic hydrocarbons. This allows for a direct comparison of excited state energies,[28] at least up to the energy where ionizations from a dense manifold of σ-MOs obscures the sharper features due to π-ionizations in the PE spectra (the EA spectra usually extend beyond that range).

In Figs. 1–3, the results of the CASPT2 calculations (at the neutral geometries for the PE spectra and at the cation geometries for the EA spectra) are schematically represented by black and white bars where the height of the black part indicates the proportion of Koopmans configurations (*i.e.* those which can be attained by ejection of an electron from a doubly occupied MO of the neutral compound *cf.* Tables 1–3) in the CASSCF wavefunction of each state. In a first approximation, these should be proportional to the contribution of these states to the intensity of the corresponding PE bands.

The results of the calculations are summarized numerically in Tables 1–3. The columns next to the excited state energies show the contribution of different excited configurations to the CASSCF wavefunctions. These contributions are indicated in terms of electron promotions between the MOs shown in Fig. 4. At the neutral geometry which pertains to the PE spectra, the contribution of Koopmans configurations is given in percent (%K) whereas for the radical cation geometry the oscillator strengths for electronic transitions are listed. Below we will elaborate on the results for parent naphthalene and its radical cation in some detail before turning to a briefer discussion of those for the two alkylated derivatives.

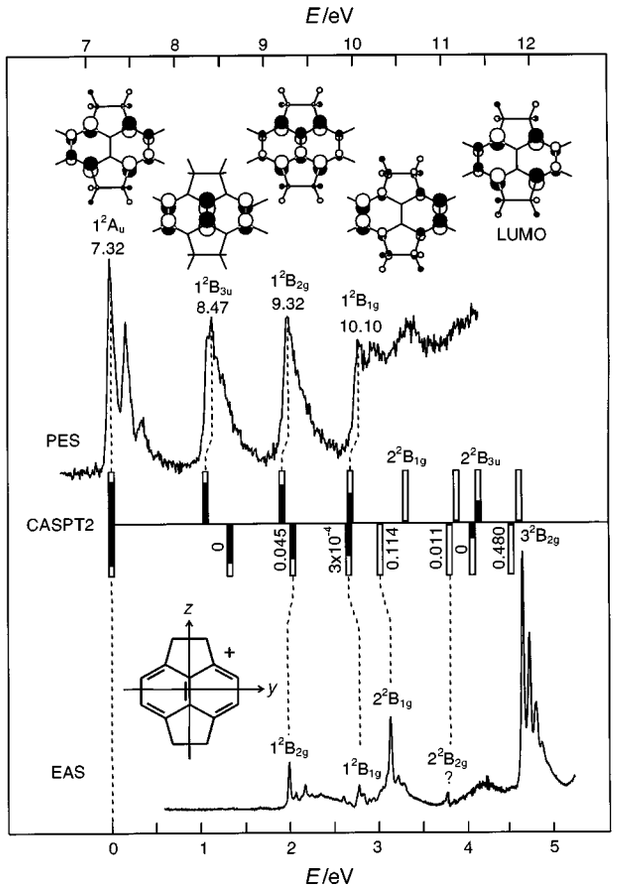

Fig. 3 Photoelectron spectrum (PES) of dihydroacenaphthylene (**A**) and electronic absorption spectrum (EAS) of the corresponding radical cation, along with a representation of the CASPT2 results listed in Table 2. For explanations, see caption to Fig. 1.

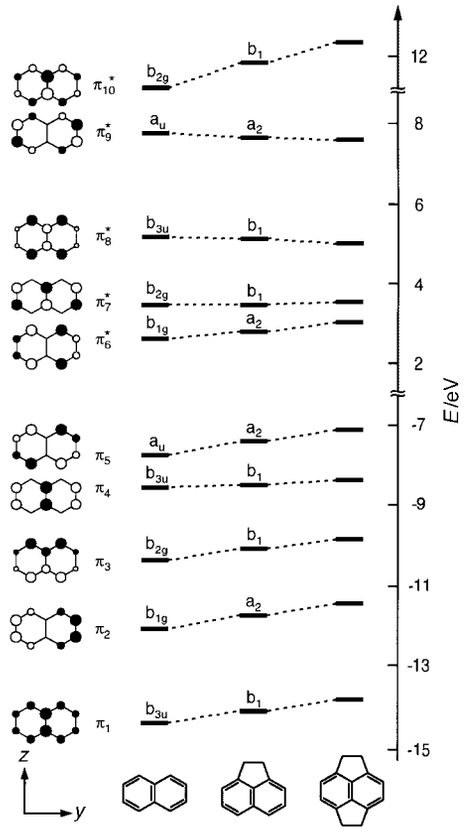

Fig. 4 Molecular orbitals π_1–π_{10}* of naphthalene, their symmetry designations in D_{2h} and C_{2v} (provided the cartesian axes are oriented as indicated in the bottom right corner) and orbital energies from a 3-21G SCF calculation on neutral **N**, **A** and **P**

Naphthalene radical cation

The radical anion and cation of naphthalene are among the most thoroughly investigated organic radical ions.[2–17] Therefore, taken individually, the two spectra in Fig. 1 represent no new information but they are presented for convenient comparison of the two experiments with the corresponding calculations which will serve in particular to highlight the excited state shifts on going from the neutral geometry to that of the radical cation.

The PE spectrum of **N** has been reported and discussed numerous times, most comprehensively by Brogli *et al.*[2] The vertical ionization energies determined in the present work coincide to ±10 meV with those reported in the above work. PE spectra are traditionally and conveniently interpreted within the framework of Koopmans' theorem[29] which provides a direct and transparent relationship between ionization energies and the energies of doubly occupied MOs ($I_{v,i} = -\varepsilon_i$). Apart from the neglect of the electron reorganization energy of the cation and the difference in correlation energies between the neutral and the radical cation (two terms which tend to cancel for valence ionizations, which is the reason for the quantitative success of this approximation), a fundamental assumption behind Koopmans' theorem is that all states under consideration are well described by single configurations which correspond to loss of a single electron from a doubly occupied MO of the neutral.

The present calculations show that this holds reasonably well for the states corresponding to the first three PE bands of **N** whereas the fourth excited state is only described to 56% by the configuration arising by ionization from the π_2 ($1b_{1g}$) orbital. This contribution may, however, lend sufficient intensity to the PE cross-section to give rise to the observed sharp feature at 10.85 eV. Above 11 eV, closely spaced states which correspond to ionizations from C–C σ-MOs begin to take over which makes it impossible to distinguish contributions from π-states, in particular 2^2B_{3u} (46% Koopmans character) which should contribute significantly to the PE cross-section around 12 eV. We note the excellent agreement between the observed $I_{v,i}$ and the excited state energies calculated by CASPT2.

Turning to the EA spectrum, we note that the band positions coincide to within 10 cm^{-1} with those reported earlier from measurements in argon.[9,10] In their comprehensive recent neon matrix study, Salama and Allamandola[10] reported (but did not show) two additional bands at 40 933 and 44 903 cm^{-1} (5.07 and 5.57 eV, respectively) which we were unable to discern clearly in our spectra. As will be shown below, CASPT2 supports the assignment of Salama and Allamandola which indicates that our measurements were perhaps not sensitive enough to observe these two weak transitions.

The literature records numerous calculations of the excited states of naphthalene radical ions. The earliest ones[14,30–32] took advantage of the fact that the pairing properties of MOs (and hence radical ion states) for alternant hydrocarbons which are an inherent property of Hückel theory prevail also in π-CI (configuration interaction) wavefunctions obtained on the basis of PPP-SCF MOs.[33] Hence, these calculations predicted identical spectra for radical anions and cations of alternant hydrocarbons, not in stark disagreement with experiment.[7] These pairing properties hold no longer if all valence electrons are correlated, such as in the open-shell versions of the popular CNDO/S[34] and INDO/S-CI methods.[35] More recently, Du *et al.* employed the latter method for a comprehensive theoretical study of $\mathbf{N}^{\bullet+}$ and $\mathbf{N}^{\bullet-}$, as well as some derivatives, which appeared to account well for the experimental data.[15] However, their calculations were based on the geometry of neutral **N**, and

Table 1 Excited states of the radical cation of naphthalene ($\mathbf{N}^{\bullet+}$), ordered by CASPT2 energies (experimental numbers in italics)

	Neutral equilibrium geometry					Radical cation equilibrium geometry				
			CASSCF[a]				CASPT2			
States	PES/eV	CASPT2/eV	eV	%K[b]	CASSCF configurations[c] (%)	EAS/eV	eV	f[d]	CASSCF/eV[a]	CASSCF configurations[c] (%)
1^2A_u	*(0)*[e]	(0)	(0)	82	82 $(\pi_5)^1$	*(0)*[e]	(0)	—	(0)	82 $(\pi_5)^1$
1^2B_{3u}	*0.73*	0.73	0.46	80	80 $\pi_4\rightarrow\pi_5$	—	0.99	0.0	0.83	79 $\pi_4\rightarrow\pi_5$
1^2B_{2g}	*1.93*	1.78	1.97	71	71 $\pi_3\rightarrow\pi_5$	*1.84*	1.89	4.2×10^{-2}	2.10	69 $\pi_3\rightarrow\pi_5$
1^2B_{1g}	*2.70*	2.65	2.90	56	56 $\pi_2\rightarrow\pi_5$ 8 $\pi_5\rightarrow\pi_6$* 6 $\pi_4\rightarrow\pi_7$*	*2.69*	2.70	2.7×10^{-3}	2.94	45 $\pi_2\rightarrow\pi_5$ 24 $\pi_5\rightarrow\pi_6$* 1 $\pi_4\rightarrow\pi_7$*
2^2B_{1g}	—	3.47	3.72	2	54 $\pi_5\rightarrow\pi_6$* 9 $\pi_4\rightarrow\pi_7$* 2 $\pi_2\rightarrow\pi_5$*	*3.25*	3.24	8.1×10^{-2}	3.54	40 $\pi_5\rightarrow\pi_6$* 13 $\pi_2\rightarrow\pi_5$ 11 $\pi_4\rightarrow\pi_7$*
2^2B_{2g}	—	4.02	4.57	1	35 $\pi_4\rightarrow\pi_6$* 29 $\pi_5\rightarrow\pi_7$*	*4.02*	3.98	1.2×10^{-1}	4.50	35 $\pi_4\rightarrow\pi_6$* 31 $\pi_5\rightarrow\pi_7$*
2^2B_{3u}	*?*	4.03	4.47	46	46 $\pi_1\rightarrow\pi_5$ 9 $\pi_5\rightarrow\pi_8$* 8 $\pi_3\rightarrow\pi_6$*	—	4.03	0.0	4.26	40 $\pi_1\rightarrow\pi_5$ 17 $\pi_5\rightarrow\pi_8$* 12 $\pi_3\rightarrow\pi_6$*
3^2B_{2g}	—	4.47	5.12	6	34 $\pi_4\rightarrow\pi_6$* 15 $\pi_5\rightarrow\pi_7$* 13 $\pi_4\rightarrow\pi_5$ + $\pi_4\rightarrow\pi_7$*	*4.55*	4.44	3.9×10^{-1}	5.17	37 $\pi_4\rightarrow\pi_6$* 14 $\pi_5\rightarrow\pi_7$* 8 $\pi_4\rightarrow\pi_5$ + $\pi_4\rightarrow\pi_7$*
3^2B_{1g}	—	4.90	5.47	0	41 $\pi_1\rightarrow\pi_7$* 22 $\pi_1\rightarrow\pi_5$ + $\pi_1\rightarrow\pi_6$*	*?*	5.09	1.7×10^{-2}	5.61	41 $\pi_4\rightarrow\pi_7$* 22 $\pi_4\rightarrow\pi_5$ + $\pi_4\rightarrow\pi_6$*
4^2B_{1g}	—	5.49	6.50	9	27 $\pi_4\rightarrow\pi_7$* 12 $\pi_4\rightarrow\pi_5$ + $\pi_4\rightarrow\pi_6$* 9 $\pi_2\rightarrow\pi_5$*	*?*	5.69	5.0×10^{-2}	6.59	26 $\pi_4\rightarrow\pi_7$* 10 $\pi_4\rightarrow\pi_5$ + $\pi_4\rightarrow\pi_6$* 7 $\pi_2\rightarrow\pi_5$*

[a] Active space: nine electrons in five occupied and five virtual π-MOs. [b] Percent Koopmans character (for explanation see text), proportional to intensity of PE band. [c] Composition of states in terms of configurations that arise by excitations among the MOs shown in Fig. 4. [d] Oscillator strength for electronic transition. [e] First ionization potential of **N**, origin of energy scale for excited states.

Table 2 Excited states of the radical cation of dihydroacenaphthylene ($\mathbf{A}^{\bullet+}$), ordered by CASPT2 energies (experimental numbers in italics)

	Neutral equilibrium geometry					Radical cation equilibrium geometry				
			CASSCF[a]				CASPT2			
States	PES/eV	CASPT2/eV	eV	%K[b]	CASSCF configurations[c] (%)	EAS/eV	eV	f[d]	CASSCF/eV[a]	CASSCF configurations[c] (%)
1^2A_2	*(0)*[e]	(0)	(0)	0	82 $(\pi_5)^1$	*(0)*[e]	(0)	—	(0)	82 $(\pi_5)^1$
1^2B_1	*0.95*	0.92	0.71	79	79 $\pi_4\rightarrow\pi_5$	*?*	1.20	5.3×10^{-6}	1.06	77 $\pi_4\rightarrow\pi_5$
2^2B_1	*1.92*	1.88	1.98	72	72 $\pi_3\rightarrow\pi_5$	*1.89*	1.99	4.5×10^{-2}	2.11	70 $\pi_3\rightarrow\pi_5$
2^2A_2	*2.55*	2.72	2.91	56	56 $\pi_2\rightarrow\pi_5$ 9 $\pi_5\rightarrow\pi_6$* 9 $\pi_4\rightarrow\pi_7$*	*2.76*	2.72	2.1×10^{-4}	2.96	37 $\pi_2\rightarrow\pi_5$ 33 $\pi_5\rightarrow\pi_6$* 3 $\pi_5\rightarrow\pi_6$*
3^2A_2	—	3.44	3.63	0	55 $\pi_5\rightarrow\pi_6$* 9 $\pi_4\rightarrow\pi_7$* 3 $\pi_2\rightarrow\pi_5$*	*3.23*	3.18	9.3×10^{-2}	3.43	34 $\pi_5\rightarrow\pi_6$* 20 $\pi_2\rightarrow\pi_5$* 15 $\pi_4\rightarrow\pi_7$*
3^2B_1	—	4.00	4.51	2	37 $\pi_5\rightarrow\pi_7$* 29 $\pi_4\rightarrow\pi_6$*	*?*	3.94	4.0×10^{-2}	4.46	35 $\pi_5\rightarrow\pi_7$* 27 $\pi_4\rightarrow\pi_6$*
4^2B_1	*?*	4.06	4.25	41	41 $\pi_1\rightarrow\pi_5$ 15 $\pi_5\rightarrow\pi_8$* 11 $\pi_3\rightarrow\pi_6$*	*?*	3.99	7.7×10^{-4}	4.27	30 $\pi_1\rightarrow\pi_5$ 22 $\pi_5\rightarrow\pi_7$* 14 $\pi_5\rightarrow\pi_8$*
5^2B_1	—	4.54	5.20	4	40 $\pi_4\rightarrow\pi_6$* 14 $\pi_4\rightarrow\pi_6$* + $\pi_4\rightarrow\pi_5$ 7 $\pi_5\rightarrow\pi_7$*	*4.56*	4.53	3.6×10^{-1}	5.23	34 $\pi_4\rightarrow\pi_6$* 16 $\pi_4\rightarrow\pi_6$* + $\pi_4\rightarrow\pi_5$ 8 $\pi_5\rightarrow\pi_7$*

[a] Active space: nine electrons in five occupied and five virtual π-MOs. [b] Percent Koopmans character (for explanation see text), proportional to intensity of PE band. [c] Composition of states in terms of configurations that arise by excitations among the MOs shown in Fig. 4. [d] Oscillator strength for electronic transition. [e] First ionization potential of **N**, origin of energy scale for excited states.

as EA spectra of radical ions are recorded at the ions' equilibrium geometry, the question of what errors were introduced by this arises.

We addressed this issue by performing for the first time separate calculations on both structures, employing the B3LYP density functional method for the geometry optimizations and the CASPT2 method for excited state calculations (*cf.* Fig. 1 and Table 1). Indeed we find that some states undergo pronounced shifts between the two geometries. Most strongly affected is the 1^2B_{3u} state (second PE band) which is, however, not observed in the EA spectrum of $\mathbf{N}^{\bullet+}$ because u→u electronic transitions are electric dipole forbidden in D_{2h}. The shift of that state to higher energies at the cation geometry can easily be understood by considering that the $1b_{3u}$ MO, π_4, is strongly bonding along C–C bonds which are weakened on ionizations (because the $1a_u$-HOMO, π_5, is antibonding along the same bonds). As the π_4 has the same nodal properties as the HOMO on the periphery of the **N** molecule, no big shift is expected (and found) for the 1^2B_{2g} state (3rd PE band of **N**, first EA band of $\mathbf{N}^{\bullet+}$).

Somewhat suprisingly, the 1^2B_{1g} state shows also only a very small shift in spite of the strongly bonding nature of the $1b_{1g}$ MO along the C2–C3 bond. However, the composition of the CASSCF wavefunction changes considerably on going from the neutral to the cation geometry (the contribution of the HOMO→LUMO excited configuration increases from

Table 3 Excited states of the radical cation of pyracene ($\mathbf{P}^{\bullet+}$), ordered by CASPT2 energies (experimental numbers in italics)

	Neutral equilibrium geometry					Radical cation equilibrium geometry				
			CASSCF[a]				CASPT2			
States	PES/eV	CASPT2/eV	eV	%K[b]	CASSCF configurations[c] (%)	EAS/eV	eV	f[d]	CASSCF/eV[a]	CASSCF configurations[c] (%)
1^2A_u	*(0)*[e]	(0)	(0)	0	83 $(\pi_5)^1$	*(0)*[e]	(0)	—	(0)	82 $(\pi_5)^1$
1^2B_{3u}	*1.15*	1.06	0.86	80	79 $\pi_4\rightarrow\pi_5$	—	1.34	0.0	1.25	77 $\pi_4\rightarrow\pi_5$
1^2B_{2g}	*2.00*	1.93	2.17	73	72 $\pi_3\rightarrow\pi_5$	*1.99*	2.05	4.5×10^{-2}	2.31	70 $\pi_3\rightarrow\pi_5$
1^2B_{1g}	*2.78*	2.70	3.00	57	57 $\pi_2\rightarrow\pi_5$ 9 $\pi_4\rightarrow\pi_7$* 7 $\pi_5\rightarrow\pi_6$*	*2.79*	2.69	3.0×10^{-4}	3.04	36 $\pi_2\rightarrow\pi_5$ 35 $\pi_5\rightarrow\pi_6$* 1 $\pi_4\rightarrow\pi_7$*
2^2B_{1g}	—	3.32	3.66	2	58 $\pi_5\rightarrow\pi_6$* 9 $\pi_4\rightarrow\pi_7$* 2 $\pi_2\rightarrow\pi_5$	*3.15*	3.03	1.1×10^{-1}	3.44	31 $\pi_5\rightarrow\pi_6$* 23 $\pi_2\rightarrow\pi_5$ 14 $\pi_4\rightarrow\pi_7$*
2^2B_{2g}	—	3.90	4.47	1	45 $\pi_5\rightarrow\pi_7$* 24 $\pi_4\rightarrow\pi_6$*	*?*	3.81	1.1×10^{-2}	4.41	44 $\pi_5\rightarrow\pi_7$* 25 $\pi_1\rightarrow\pi_6$*
2^2B_{3u}	*?*	4.14	4.40	38	38 $\pi_1\rightarrow\pi_5$ 18 $\pi_5\rightarrow\pi_8$* 11 $\pi_3\rightarrow\pi_6$*	—	4.07	0.0	4.38	29 $\pi_5\rightarrow\pi_8$* 27 $\pi_1\rightarrow\pi_5$ 15 $\pi_3\rightarrow\pi_6$*
3^2B_{2g}	—	4.60	5.38	6	43 $\pi_4\rightarrow\pi_6$* 15 $\pi_4\rightarrow\pi_5$ + $\pi_4\rightarrow\pi_7$*	*4.65*	4.52	4.8×10^{-1}	5.47	48 $\pi_4\rightarrow\pi_6$* 9 $\pi_4\rightarrow\pi_5$ + $\pi_4\rightarrow\pi_7$*
3^2B_{1g}	—	5.08	5.74	1	39 $\pi_4\rightarrow\pi_7$* 21 $\pi_4\rightarrow\pi_5$ + $\pi_4\rightarrow\pi_6$*	*?*	5.26	1.4×10^{-2}	5.94	37 $\pi_4\rightarrow\pi_7$* 22 $\pi_4\rightarrow\pi_5$ + $\pi_4\rightarrow\pi_6$*

[a] Active space: nine electrons in five occupied and five virtual π-MOs. [b] Percent Koopmans character (for explanation see text), proportional to intensity of PE band. [c] Composition of states in terms of configurations that arise by excitations among the MOs shown in Fig. 4. [d] Oscillator strength for electronic transition. [e] First ionization potential of **N**, origin of energy scale for excited states.

Table 4 Dipole moments for selected electron excitations in the radical cations of naphthalene, pyracene and acenaphthylene

		Naphthalene		Pyracene		Acenaphthylene	
	Excitation	μ[a]	C[b]	μ[a]	C[b]	μ[a]	C[b]
2^2B_{2g}	$\pi_5\rightarrow\pi_7$*	2.10	0.56	2.12	0.67	2.03	0.49
	$\pi_4\rightarrow\pi_6$*	−3.07	0.60	−2.93	0.50	−2.58	0.45
	Weighted sum[c]	0.81		0.06		0.25	
1^2B_{1g}	$\pi_5\rightarrow\pi_6$*	1.58	−0.50	1.73	−0.61	1.60	−0.59
	$\pi_2\rightarrow\pi_5$	1.77	0.66	1.85	0.59	1.80	0.58
	Weighted sum[c]	0.47		0.05		0.17	
2^2B_{1g}	$\pi_5\rightarrow\pi_6$*	1.58	0.64	1.73	0.56	1.60	0.56
	$\pi_2\rightarrow\pi_5$	1.77	0.37	1.85	0.49	1.80	0.47
	Weighted sum[c]	2.26		2.51		2.38	

[a] Transition dipole moment. [b] CI-coefficient with which the excited configuration listed to the left enters into the (9,10)CASSCF excited state wavefunction. [c] Sum of $|\mu\times C|$ for the above pair of excited configurations, renormalized by multiplication with $(C_1^2+C_2^2)^{-\frac{1}{2}}$.

8 to 24%!) which indicates that the coincidence of EA and PE bands at this energy is due to fortuitously cancelling effects.

The right half of Table 1 shows that the second $^2B_{1g}$ state, which gives rise to the rather broad band peaking at 3.28 eV, is composed of the same two leading configurations as 1^2B_{1g}, $\pi_2\rightarrow\pi_5$ and $\pi_5\rightarrow\pi_6$*, so the question arises why the two bands have such different intensity. The answer lies in the sign of the CI-coefficients for these two configurations which is opposite in 1^2B_{1g} and similar in 2^2B_{1g} (see Table 4). Thus, the dipole moments for the $\pi_2\rightarrow\pi_5$ and for the $\pi_5\rightarrow\pi_6$* excitations, which are similar in magnitude, tend to cancel in the $1^2A_u\rightarrow1^2B_{1g}$ and reinforce each other for the $1^2A_u\rightarrow2^2B_{1g}$ transition, thus giving rise to a pair of bands of disparate intensity. This situation is reminiscent of the one prevailing in polyene radical cations[19,36] which show a similar pattern of bands for the same reason.

At this point we should, however, insert a cautionary remark: the preceding discussion, in particular with regard to the composition of states in terms of configurations, should be regarded as qualitative because, although the molecular orbitals used to describe states of different symmetry are similar to one another, they are not identical. It is also worth noting that, because the MCSCF procedure includes orbital optimization, the CI coefficients may also differ as compared to CI calculations using a single determinant reference function and one common set of orbitals for all states and symmetries. For the above reasons, a quantitative comparison of CI coefficients obtained by the different approaches is, in general, not possible. Nevertheless we note that in the higher excited states, doubly excited configurations (which are usually neglected in the semiempirical CI schemes) begin to come into play, which may explain in part why accord between experiment and CASSCF/CASPT2 is far better for high-lying excited states of $\mathbf{N}^{\bullet+}$ than it was in the previous semiempirical CI calculations.[15]

Turning to the two groups of sharp UV bands of $\mathbf{N}^{\bullet+}$ we note the unusual pattern of the vibrational progressions of the first one extending from 4.0 to 4.3 eV. The CASPT2 calculations leave no doubt that only a single dipole allowed transition occurs in this region, *i.e.* $A_u\rightarrow2^2B_{2g}$. However, they predict that the 2^2B_{3u} is nearly degenerate with the 2^2B_{2g} state with which it can mix on distortion to C_{2v} symmetry along b_{1u} normal modes. Thus, vibronic coupling effects could well be responsible for the peculiar Franck–Condon envelope of this band. In contrast, the band peaking at 4.49 eV shows a single vibrational progression with a normal intensity pattern. This band must be associated with the 3^2B_{2g} state which corresponds predominantly to excitations from the HOMO and from doubly occupied to virtual MOs (so-called B- and C-type excitations, respectively[37]).

Finally we note that CASPT2 predicts two more transitions at 5.1 and 5.7 eV, in agreement with the recent calculations,[15,16] albeit at slightly lower energies. These would appear to correspond to bands reported at 5.07 and 5.56 eV, respectively, by Salama and Allamandola.[10] The first of these could possibly have escaped detection in our experiment due to its feeble oscillator strength whereas the second one corresponds perhaps to

the shoulder at 5.5 eV on the onset of the strong $^1A_g(S_0)\rightarrow$ $^1B_{3u}(S_3)$ absorption of neutral **N** which exceeds the dynamic range of our spectrometer and could hence not be subtracted correctly.

In conclusion of this discussion of the parent naphthalene radical cation we can say that the CASPT2 predictions are generally in excellent quantitative agreement with the experimentally determined excited state energies, both at the neutral and at the cation geometries of **N**. Some of the remaining discrepancies in the positions of the UV bands arise probably from solvation effects which are not accounted for by the calculations, but as the differences are well within the usual precision of the CASPT2 predictions (±0.2 eV), we cannot draw any conclusions with regard to solvation effects. As for the nature of the excited state wavefunctions, we note that strong configurational mixing occurs above 3 eV, and that doubly excited configurations make significant contributions.

Acenaphthylene and pyracene radical cations

The PE spectrum of **A** has been measured by Heilbronner *et al.*[38] whereas that of **P** has not been reported previously. However, both radical cations have been investigated by EPR spectroscopy[39–41] which shows that a part of the unpaired spin appears in the dimethylene bridges (the hyperfine couplings to the CH_2 protons are 13–14 G in both cations, in accord with those predicted by our B3LYP calculations). Also, peak positions in the EA spectrum have been reported for $\mathbf{A}^{\bullet+}$.[42]

Inspection of Figs. 2 and 3 shows that the EA spectra of $\mathbf{A}^{\bullet+}$ and $\mathbf{P}^{\bullet+}$ below 4 eV have the same general appearance as that of $\mathbf{N}^{\bullet+}$, with only slight shifts in the band positions. Also, the intense UV band at *ca.* 4.5 eV appears with very similar shape and intensity. These features are also borne out by the CASSCF/CASPT2 calculations which show that the relative energies as well as the configurational composition of the first four excited states, as well as of the sixth one at *ca.* 4.5 eV, change little on going from $\mathbf{N}^{\bullet+}$ to $\mathbf{A}^{\bullet+}$ or $\mathbf{P}^{\bullet+}$. In particular, no excited configurations involving MOs localized predominantly to the dimethylene bridges participate in these excited states. Therefore, the only influence of these bridges is an inductive one which leads to a shift of the bands by a few tenths of an eV (to higher energies in the first three excited states, and to lower energies in the fourth one, corresponding to the third EA band).

Some of these shifts can be readily explained on the basis of first-order changes in MO energies on introduction of the dimethylene bridges (*cf.* Fig. 4). For example this leads to a rise in $\varepsilon(\pi_5)$ whereas it hardly affects π_4 which has nodes at the substitution sites; therefore the gap between those two MOs, and hence that between the two first PE-bands, widens by about 0.2 eV on introduction of each dimethylene bridge. A similar argument can be made for the blue shift of the intense 4.5 eV EA transition which is dominated by $\pi_4\rightarrow\pi_6^*$ excitation in all three radical cations (*cf.* Tables 1–3): again this shift reflects the widening of the gap between the two orbitals on alkyl substitution in the *peri* positions. Other changes, for example the red shift of the third EA band, cannot be rationalized on this simple level, because several excitations contribute to this transition, and their relative weights change on substitution.

In stark contrast to the above noted general agreement between the three EA spectra, the sharp band at 4.0–4.3 eV in $\mathbf{N}^{\bullet+}$ which corresponds to $1^2A_u\rightarrow2^2B_{2g}$ excitation seems to have all but disappeared in the two alkyl derivatives, a phenomenon which obviously calls for an explanation. To this end we calculated the two transition dipole moments for the excitations $\pi_4\rightarrow\pi_6^*$ and $\pi_5\rightarrow\pi_7^*$ which constitute the major components of the $1^2A_u\rightarrow2^2B_{2g}$ excitation in $\mathbf{N}^{\bullet+}$ and $\mathbf{P}^{\bullet+}$, and in the analogous $1^2A_2\rightarrow4^2B_1$ excitation in $\mathbf{A}^{\bullet+}$ (*cf.* Tables 1–3). In accord with the fact that the orbitals π_4–π_7^* involved in these transitions are mainly localized in the naphthalene moieties of $\mathbf{A}^{\bullet+}$ and $\mathbf{P}^{\bullet+}$, these transition moments change little between the three compounds (see Table 4).

However, as can be verified easily by inspection of the MOs in Fig. 4, the transition moments for the $\pi_4\rightarrow\pi_6^*$ and the $\pi_5\rightarrow\pi_7^*$ excitations are oriented in an *antiparallel* way along the *y*-axis. Since the CI-coefficients of the two excited states in the CASSCF wavefunction have equal signs, the two transition moments have a tendency to cancel at the CASSCF level.[43] When the transition dipole moments are weighted by the CI coefficients of the corresponding excited states in the CASSCF wavefunction, their sum (after renormalization) reflects indeed the observed strong decrease of the band intensity on going from $\mathbf{N}^{\bullet+}$ to $\mathbf{P}^{\bullet+}$ (note that the integrated band intensity is proportional to the *square* of the transition dipole moment which differs by a factor of nearly 200 between the two compounds!). The weighted sum of the two transition moments is larger for $\mathbf{A}^{\bullet+}$, but then we cannot expect this crude two-state model to give quantitative accord with experiment.

When the oscillator strengths are calculated on the basis of the full CASSCF wavefunctions and CASPT2 energy differences (see Tables 1–3), they fall from 0.12 for $\mathbf{N}^{\bullet+}$ *via* 0.04 for $\mathbf{A}^{\bullet+}$ to 0.01 for $\mathbf{P}^{\bullet+}$. Our failure to detect these bands in $\mathbf{A}^{\bullet+}$ and $\mathbf{P}^{\bullet+}$ seems to indicate that the quantitative accuracy of these calculated transition moments leaves room for improvement, *i.e.* the oscillator strengths predicted for the two alkylated derivatives, in particular for $\mathbf{A}^{\bullet+}$, are certainly too high. However, as we have shown above, these oscillator strengths result from small differences between comparatively large numbers, and they depend very critically on the relative magnitude of the two CI-coefficients which are for example quite sensitive to the size of the active space. Therefore, this lack of quantitative agreement with experiment is not unexpected and should not be overemphasized. More importantly, our calculations led us to an understanding of the reason for the 'disappearance' of a prominent EA band in $\mathbf{N}^{\bullet+}$ on introducing alkyl bridges.

It would be interesting to see what happens to this transition in other naphthalene derivatives. The only other such compound which we have recently investigated, is the cyclobutaderivative of $\mathbf{A}^{\bullet+}$.[44] The EA spectrum of this cation up to 4 eV shows great similarity to that of $\mathbf{A}^{\bullet+}$, except that the second and third band are broader, due to the participation of cyclobutane σ-MOs which lead to larger relaxation energies in the corresponding states of the radical cation. Unfortunately, the range of observation in the case of these experiments did not extend beyond 4 eV, so we could not determine the fate of the optical transition corresponding to the $\pi_4\rightarrow\pi_6^*$ and the $\pi_5\rightarrow\pi_7^*$ excitations in this compound.

Summary and conclusions

We have presented a complete analysis of the electronic structure of the naphthalene radical cation, comprising excited states up to 5.5 eV. The nature of these excited states is discussed on the basis of CASSCF calculations which permit detailed insight into the electronic structures in terms of the π molecular orbitals of naphthalene. In addition, we investigated derivatives containing one or two dimethylene bridges in the *peri* positions of the naphthalene rings. The results of the corresponding observations and calculations are summarized graphically in Fig. 5. This shows that the introduction of alkyl bridges has only a minor influence on the excited state energies of the corresponding radical cations. The same holds for the intensity and shape of most of the absorption bands shown in Figs. 1–3, with one notable exception: the sharp absorption band of the naphthalene radical cation at *ca.* 4 eV is impossible to discern in the spectra of the alkyl derivatives. CASSCF calculations show that it is the *intensity* of this band which changes drastically on alkyl substitution, not its position. This is due to a cancellation of transition moments for constituent one-electron excitations that is incomplete in naphthalene, but becomes nearly complete the alkyl derivatives.

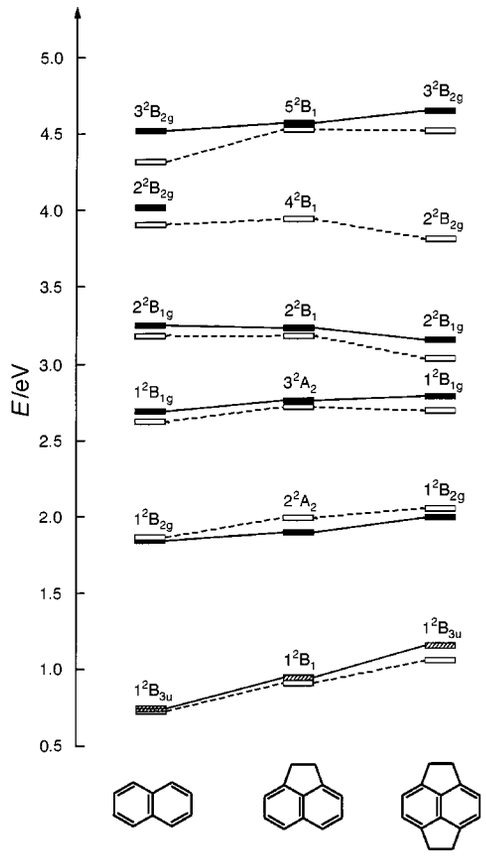

Fig. 5 Correlation diagram of the different excited states of $\mathbf{N}^{\bullet+}$, $\mathbf{A}^{\bullet+}$ and $\mathbf{P}^{\bullet+}$, as obtained from experiment (hashed bars: PE spectra, black bars: EA spectra) and CASPT2 calculations (open bars: at neutral geometry, to be compared with hashed bars, white bars: at cation geometry, to be compared to black bars). Note that the energy scale is spread between 0 and 2 eV to better show the differences between the two experiments/geometries.

Acknowledgements

The research reported in this work has been supported through grants from the Swiss National Science Foundation (Project No. 2028–047212.96) and the Swedish Natural Science Research Council (NFR). We would like to thank Professor Jakob Wirz (University of Basel) for a gift of samples of **A** and **P**, and we are very indebted to the group of Professor Michael Allan (University of Fribourg) for measuring the photoelectron spectra.

References

1 F. Salama and L. J. Allamandola, *Adv. Space Res.*, 1994, **15**, 413.
2 F. Brogli, E. Heilbronner and T. Kobayashi, *Helv. Chim. Acta*, 1972, **55**, 274.
3 R. C. Dunbar and R. Klein, *J. Am. Chem. Soc.*, 1976, **98**, 7994.
4 Y.-P. Hi, Y.-C. Yang, S. J. Klippenstein and R. C. Dunbar, *J. Phys. Chem.*, 1995, **99**, 12 115.
5 M. C. R. Cockett, H. Ozeki, K. Okuyama and K. Kimura, *J. Chem. Phys.*, 1993, **98**, 7763.
6 R. Erickson, N. P. Benetis, A. Lund and M. Lindgren, *J. Phys. Chem. A*, 1997, **101**, 2390.
7 T. Shida, *Electronic Absorption Spectra of Organic Radical Ions*, Elsevier, Amsterdam, 1988.
8 R. Gschwind and E. Haselbach, *Helv. Chim. Acta*, 1979, **62**, 941.
9 L. Andrews, B. J. Kelsall and T. A. Blankenship, *J. Phys. Chem.*, 1982, **86**, 2916.
10 F. Salama and L. J. Allamandola, *J. Chem. Phys.*, 1991, **94**, 6964.
11 J. Szczepanski, D. Roser, W. Personette, M. Eyring, R. Pellow and M. Vala, *J. Phys. Chem.*, 1992, **96**, 7876.
12 D. M. Hudgins, S. A. Sandford and L. J. Allamandola, *J. Phys. Chem.*, 1994, **98**, 4243.
13 P. Jorgensen and J. C. Poulsen, *J. Phys. Chem.*, 1974, **78**, 1420.
14 R. Zahradnik, P. Carsky and Z. Slanina, *Collect. Czech. Chem. Commun.*, 1973, **38**, 1886.
15 P. Du, F. Salama and G. H. Loew, *Chem. Phys.*, 1993, **173**, 421.
16 C. Niederalt, S. Grimme and S. D. Peyerimhoff, *Chem. Phys. Lett.*, 1995, **245**, 455.
17 B. O. Roos, K. Andersson, M. P. Fülscher, P.-Å. Malmqvist and L. Serrano-Andrés, *Adv. Chem. Phys.*, 1996, **93**, 219.
18 B. O. Roos, M. P. Fülscher, P.-Å. Malmqvist, M. Merchàn and L. Serrano-Andrés, in *Quantum Mechanical Electronic Structure Calculations with Chemical Accuracy*, ed. S. R. Langhoff, Kluwer, Dordrecht, 1994.
19 M. P. Fülscher, S. Matzinger and T. Bally, *Chem. Phys. Lett.*, 1995, **236**, 167.
20 L. Truttmann, K. R. Asmis and T. Bally, *J. Phys. Chem.*, 1995, **99**, 17 844.
21 T. Bally, in *Radical Ionic Systems* (*Topics in Molecular Organization and Engineering*), eds. A. Lund and M. Shiotani, Kluwer, Dordrecht, 1991, vol. 6, pp. 3–54.
22 R. Dressler, L. Neuhaus and M. Allan, *J. Electron Spectrosc. Relat. Phenom.*, 1983, **31**, 181.
23 B. G. Johnson, P. M. W. Gill and J. A. Pople, *J. Chem. Phys.*, 1993, **98**, 5612.
24 M. J. Frisch, G. W. Trucks, H. B. Schlegel, P. M. W. Gill, B. G. Johnson, M. A. Robb, J. R. Cheeseman, T. Keith, G. A. Petersson, J. A. Montgomery, K. Raghavachari, M. A. Al-Laham, V. G. Zakrzewski, J. V. Ortiz, J. B. Foresman, J. Cioslowski, B. B. Stefanov, A. Nanayakkara, M. Challacombe, C. Y. Peng, P. Y. Ayala, W. Chen, M. W. Wong, J. L. Andres, E. S. Repogle, R. Gomperts, R. L. Martin, D. J. Fox, J. S. Binkley, D. J. DeFrees, J. Baker, J. P. Stewart, M. Head-Gordon, M. C. Gonzales and J. A. Pople, Gaussian Program, GAUSSIAN94, Rev. B1 and D4; Gaussian, Inc., Pittsburgh, PA, 1995.
25 K. Andersson and B. O. Roos, in *Modern Electronic Structure Theory*, *Part I* (*Advanced Series in Physical Chemistry*), ed. D. R. Yarkony, Word Scientific, Singapore, 1995, vol. 2, p. 55.
26 K. Andersson, M. R. A. Blomberg, M. P. Fülscher, V. Kellö, R. Lindh, P.-Å. Malmqvist, J. Noga, J. Olson, B. O. Roos, A. Sadlej, P. E. M. Siegbahn, M. Urban and P.-O. Widmark, MOLCAS, 3rd edn., University of Lund, Sweden, 1994.
27 P.-O. Widmark, P.-Å. Malmqvist and B. O. Roos, *Theor. Chim. Acta*, 1990, **77**, 291.
28 Note that this does not imply that the radical cations do not change their energy on relaxing from the neutral to the cation geometry. In fact, both B3LYP and CASPT2 calculations agree that this relaxation energy amounts to about 0.1 eV (all energies available in the supporting information).
29 T. Koopmans, *Physica*, 1934, **7**, 104.
30 G. J. Hoijtink, N. H. Verlhorst and P. J. Zandstra, *Mol. Phys.*, 1960, **3**, 533.
31 A. Hinchcliffe, J. N. Murrell and N. Trinajstic, *Trans. Faraday Soc.*, 1966, **62**, 1362.
32 A. Ishitani and S. Nagakura, *Theor. Chim. Acta*, 1966, **4**, 236.
33 A. D. McLachlan, *Mol. Phys.*, 1959, **2**, 271.
34 H. M. Chang, H. H. Jaffe and C. A. Masmanides, *J. Phys. Chem.*, 1975, **79**, 1118.
35 M. C. Zerner and J. E. Ridley, *Theor. Chim. Acta*, 1973, **32**, 111.
36 T. Bally, S. Nitsche, K. Roth and E. Haselbach, *J. Am. Chem. Soc.*, 1984, **106**, 3927.
37 R. Zahradnik and P. Carsky, *J. Phys. Chem.*, 1970, **74**, 1235.
38 E. Heilbronner, T. Hoshi, J. L. v. Rosenberg and K. Hafner, *Nouv. J. Chim.*, 1976, **1**, 105.
39 A. C. Buchanan, R. Livingston, A. S. Dworkin and G. P. Smith, *J. Phys. Chem.*, 1980, **84**, 423.
40 A. Terahara, H. Ohya-Nishigushi, N. Hirota and A. Oku, *J. Phys. Chem.*, 1986, **90**, 1564.
41 A. G. Davies and D. C. McGuchan, *Organometallics*, 1991, **10**, 329.
42 L. Andrews, R. S. Friedman and B. J. Kelsall, *J. Phys. Chem.*, 1985, **89**, 4550.
43 Note that the phases of one of the MOs that are involved in these excitations could have been chosen differently, such that the transition moments are oriented parallel. However, this would necessarily have entailed a change in sign of one of the two CI-coefficients such that the net result would remain unaffected by this (arbitrary) phase change.
44 Z. Zhu, T. Bally, J. Wirz and M. Fülscher, *J. Chem. Soc.*, *Perkin Trans. 2*, 1998, 1083.

Paper 8/02861C
Received 16*th April* 1998
Accepted 3*rd June* 1998